A Technique for Eliminating Water Returns from Lidar Beach Elevation Surveys

MARISSA L. YATES AND R. T. GUZA

Scripps Institution of Oceanography, La Jolla, California

ROBERTO GUTIERREZ

The University of Texas at Austin, Austin, Texas

RICHARD SEYMOUR

Scripps Institution of Oceanography, La Jolla, California

(Manuscript received 7 March 2007, in final form 15 February 2008)

ABSTRACT

Airborne light detecting and ranging (lidar) systems can survey hundreds of kilometers of shoreline with high spatial resolution (several elevation estimates per square meter). Sequential surveys yield spatial change maps of beach and dune sand levels. However, lidar data include elevations of the exposed, subaerial beach and, seaward of the waterline, the ocean surface. Here, a simple method is developed to find the waterline and eliminate returns from the ocean surface. A vertical elevation cutoff is used, with the waterline elevation (W) above the known tide level because of the superelevation from wave setup and runup. During each lidar pass, the elevation cutoff (W) is assumed proportional (C) to the offshore significant wave height H_s. Comparison of in situ and lidar surveys on a moderately sloped, dissipative California beach yields $C \approx 0.4$, which is qualitatively consistent with existing observations of runup and setup. The calibrated method rejects ocean surface data, while retaining subaerial beach points more than 70 m seaward of the mean high waterline, which is often used as a conservative default waterline.

1. Introduction

Beach survey methods have evolved rapidly with the use of kinematic global positioning system (GPS) techniques (Morton et al. 1993). Airborne light detecting and ranging (lidar) systems (Brock et al. 2002) survey hundreds of kilometers of shoreline with high spatial resolution in a few days. With swath widths of a few hundred meters, coastal lidar surveys map the offshore ocean surface, the subaerial beach face, and the backbeach (e.g., cliffs, seawalls, landward development). Lidar surveys spanning long coastal reaches are a unique resource for studying variability across the entire exposed beach system. Repeated surveys can be used to monitor changes in shorelines (Stockdon et al. 2002), beaches and dunes (Saye et al. 2005; Woolard and Colby 2002), and sea cliffs (Sallenger et al. 2002; Young and Ashford 2006). Additionally, lidar surveys have been used to quantify beach changes after a beach nourishment (Gares et al. 2006), after hurricanes (Zhang et al. 2005; Robertson et al. 2007), and during an El Niño event (Revell et al. 2002). Based on concurrent airborne lidar and ground-based beach surveys, root-mean-square (RMS) vertical lidar errors are about 15 cm (Sallenger et al. 2003), and RMS horizontal errors in the cross-shore location of the mean high-water (MHW) vertical datum are about 2.5 m on a moderately sloped beach (Stockdon et al. 2002).

Lidar data include elevations of the subaerial beach and, seaward of the waterline, the ocean surface. The waterline location depends on the local bathymetry and the tide and wave conditions. For small alongshore reaches at specific study sites, the exposed beach points have been identified manually (Woolard and Colby 2002; Shrestha et al. 2005). However, for surveys of large alongshore distances, automated methods are needed to remove ocean surface data. Stockdon et al. (2002) used differences between multiple lidar passes to

Corresponding author address: Marissa L. Yates, Scripps Institution of Oceanography, 9500 Gilman Drive, La Jolla, CA 92093. E-mail: myates@coast.ucsd.edu

DOI: 10.1175/2008JTECHO561.1

locate the shoreline. When all passes over a given area yielded similar elevations, the area was assumed to be subaerial beach. When independent passes yielded significantly different elevations, the differences were ascribed to the variation between passes of the location of wave crests and troughs, and the area was classified as water. The method requires more than one pass and is less effective when wave heights are low and their effect is difficult to detect near the waterline.

Here, nearly concurrent lidar and in situ surveys (described in section 2) are used to calibrate and test a simple method (section 3) that, using lidar data and independently known tides and waves, estimates the seaward limit of subaerial beach lidar data points (e.g., the waterline location) in each pass. The tuned algorithm excludes ocean surface data while retaining most subaerial beach data (section 4). The results are discussed in section 5 and summarized in section 6.

2. Observations

Five nearly concurrent in situ and lidar surveys were collected at Torrey Pines State Beach, California, between September 2002 and April 2005 (Fig. 1; Table 1). The in situ surveys measured the elevation of the beach face shoreward of the waterline and the elevation of the seabed seaward of the waterline, whereas the lidar surveys measured the elevation of the ocean surface seaward of the waterline (Figs. 1c,d, 3c, 4c, 6c). For each lidar pass, the in situ and lidar surveys diverge seaward of the waterline. These divergence waterlines, based on in situ and lidar surveys, are used to calibrate the method that uses tides and wave heights to locate the waterline position in lidar surveys.

a. Study site

Torrey Pines State Beach (32.9°N, 117.26°W) is a relatively wide, sandy beach backed by high cliffs in most locations. The distance from the backbeach (e.g., seawall or cliff) to mean sea level (MSL) varied between about 20 and 150 m, with slopes near MSL between about 0.01 and 0.04 (Figs. 1c, 3c, 4c, 6c). The sandy beach face, with median grain diameter of 0.2 mm (Seymour et al. 2005), sometimes contained a few cobbles.

The tide level was measured every 6 min at the Scripps Institution of Oceanography (SIO) pier [National Oceanic and Atmospheric Administration (NOAA) station 9410230, located less then 1 km south of the survey region]. The significant wave height was measured at the Torrey Pines Outer Buoy, operated by the Coastal Data Information Program (CDIP). The buoy was located in 550-m water depth, about 10 km offshore of Torrey Pines State Beach, and wave heights were reported every 30 min. The nearest in time wave height and tide level were used, and the conditions during each survey are shown in Table 1.

b. Lidar surveys

Each lidar survey included the 80-km stretch of coastline from Point La Jolla (south) to Dana Point (north). The in situ survey site, Torrey Pines State Beach, is located approximately 5 km north of Point La Jolla. The Optech, Inc., Airborne Laser Terrain Mapper (ALTM) 1225 was used in conjunction with geodetic quality GPS airborne and ground-based receivers. For the September and December 2002 surveys, the ALTM 1225 was installed in a single engine Cessna 206. The later surveys (April and September 2004 and April 2005) used a twin engine Partenavia P-68 Observer.

The laser pulses at 25 kHz and scans at 26 Hz, with a scanning angle of $\pm 20°$. The near-infrared laser has a wavelength of 1024 nm, which is unable to penetrate more than a few centimeters below the ocean surface (Mobley 1994), effectively mapping the exposed beach and ocean surface, whereas green lasers are able to penetrate the water column (Guenther et al. 2000). The swath width was a few hundred meters and was determined by the altitude of the aircraft, which ranged from 320 m (when flying under low clouds) to 1150 m. The ground speed ranged from about 80 to 130 kt (40–70 $\mathrm{m\ s^{-1}}$).

The instrument platform orientation was obtained with an inertial measurement unit (IMU) containing three accelerometers and gyroscopes to measure the aircraft pitch, roll, and yaw. The aircraft position was determined using GPS trajectories and IMU outputs to calculate an aided-inertial navigation system solution. Elevation data were determined using the laser ranges and scan angles, the platform position and orientation, and calibration data and mounting parameters (Wehr and Lohr 1999). The elevation processing and quality control, including eliminating reflections from birds, beach goers, and other extraneous targets, were completed at The University of Texas at Austin Center for Space Research (and formerly in the Bureau of Economic Geology).

Each pass of the scanning lidar mapped a few hundred meter–wide swath along the coastline. Multiple, overlapping passes ensured complete coverage of the subaerial beach. Each Torrey Pines lidar survey included between three and five passes (Table 1), collected during one or two successive lower low tides (Fig. 1c). Aerial photography helped identify and exclude cliffs, revetments, piers, and seawalls from the

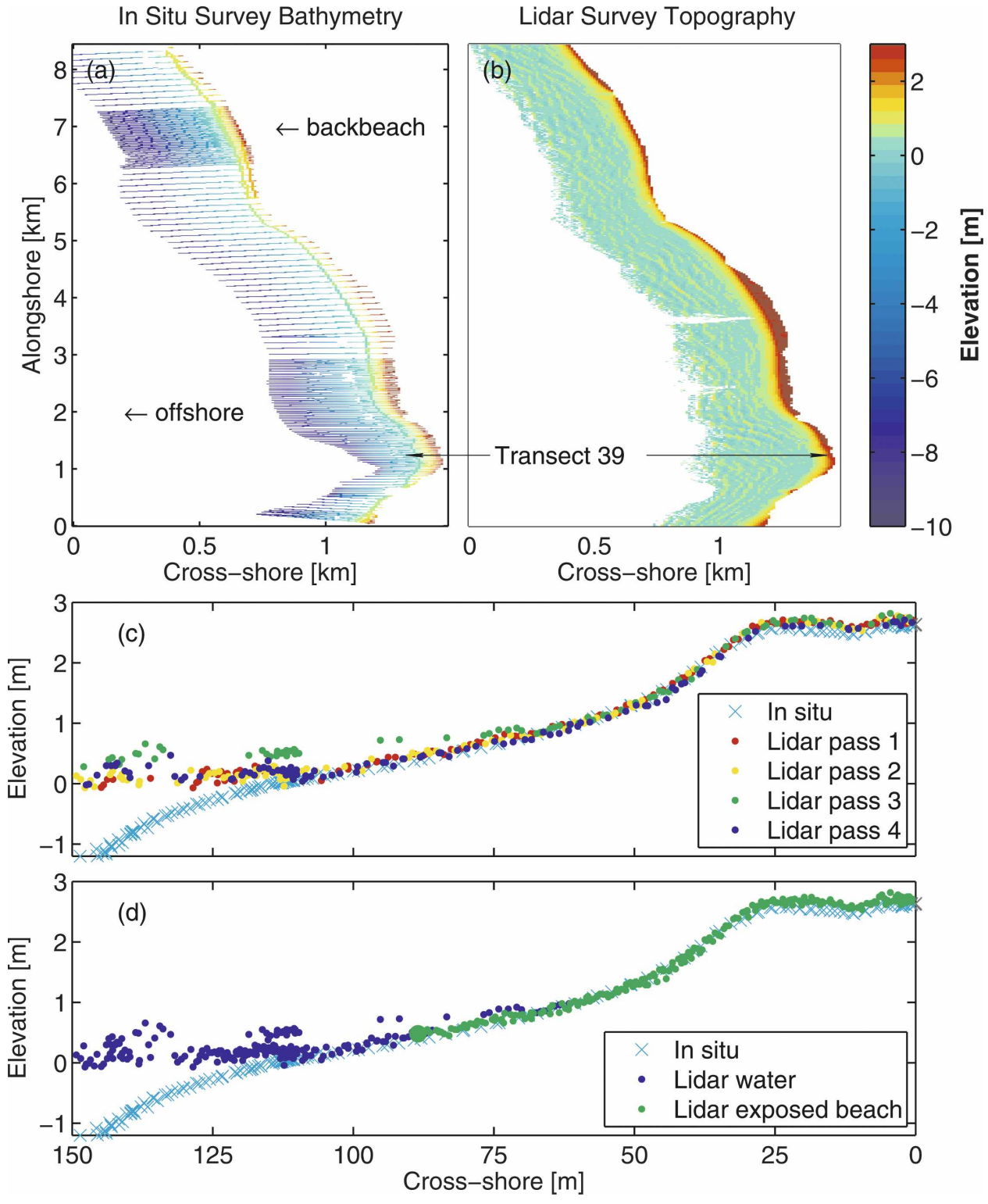

FIG. 1. Surveys of September 2004: (a) in situ bathymetry, 199 cross-shore oriented transects, extending from 10-m depth offshore to the backbeach, and (b) lidar topography, one pass shown with wave crests visible in the offshore region and the subaerial beach a narrow, red strip. Color scale is to the right. (c) Elevation vs cross-shore location on survey transect 39: in situ (blue x) and four lidar passes (colored circles; see legend). The location of the ocean surface varies between passes due to surface waves and changing tide levels. The first two passes were completed at lower low tide on 28 Sep 2004, and the next two passes were completed about 24 h later. (d) Elevation vs cross-shore location on transect 39: in situ (blue x) and lidar, all passes combined, separated using $C = 0.4$ in (1) into lidar water (dark blue) and subaerial beach (green). The large green circle is the most seaward lidar subaerial beach point. For clarity, every other data point is shown in (c) and (d).

TABLE 1. For each survey, lidar survey dates and number of passes, in situ survey dates and number of cross-shore transects, net vertical offset, tide level range [relative to North American Vertical Datum of 1988 (NAVD88)], and significant wave height range are shown.

Lidar surveys	Passes	In situ surveys	Transects	Vertical offset (cm)	Tide level (m)	Wave height (m)
9 Sep 2002	3	9–12 Sep 2002	65	11.8	0.09 to 0.19	1.2–1.3
3–4 Dec 2002	3	3–4 Dec 2002	65	15.8	−0.29 to 0.40	0.5–0.6
2 Apr 2004	4	3–6 Apr 2004	199	3.5	−0.11 to 0.14	1.2–1.3
28–29 Sep 2004	5	27–30 Sep 2004	199	1.7	0.1 to 0.68	0.9–1.0
4 Apr 2005	4	4–7 Apr 2005	199	1.0	−0.32 to −0.02	1.2–1.4

lidar data. The retained lidar data included both the subaerial sandy beach and the wavy ocean surface (Fig. 1b).

c. *In situ surveys*

In situ surveys were completed on approximately cross-shore-oriented survey transects, separated by 20–100 m in the alongshore at Torrey Pines State Beach (Fig. 1a). At low tide, a GPS-equipped all-terrain vehicle and a hand-pushed dolly surveyed the beach to wading depths. During high tide, a GPS and sonar-equipped personal watercraft surveyed each transect from 10-m water depth to as far onshore as the sonar could locate the seafloor in breaking waves. Nearly all of the in situ data used here were collected with the all-terrain vehicle and the dolly, which are more accurate than the personal watercraft system.

The first two surveys contained 65 cross-shore transect lines spanning 2 km of coastline, and the remaining surveys were extended to 199 lines spanning 8 km (Table 1). In situ surveys with 199 transects (Fig. 1a) took 3–4 days to complete, sampling during successive lower low (exposed beach) and higher high (offshore bathymetry) tides. Lidar and in situ surveys often overlap for at least one low tide and have a maximum offset of a few days (Table 1).

In situ and lidar data were compared along cross-shore profiles constructed using the in situ data points within 10 m alongshore of predefined survey transects. Alongshore offsets are due to human sampling error in the in situ surveys. Corresponding lidar points were defined as those within 1 m of each in situ point (Figs. 1c,d, 3c, 4c, 6c, 7b–d).

3. Finding the waterline in lidar data

a. *Using tides and waves*

The vertical elevation of the waterline (Fig. 2) was determined by tides, wave setup (a steady superelevation resulting from breaking waves), and wave runup (oscillations about the mean waterline due to individual waves and wave groups). There are many formulations for the dependence of setup and runup on incident wave conditions and beach morphology. Accurate, dynamically based predictions of setup and runup at the shoreline require bathymetry across the entire surf zone, but this information is rarely, if ever, available for the long coastal reaches surveyed with lidar systems. A simple relationship for the maximum vertical waterline elevation (W) above the tide level, not dependent on bathymetry or details of the wave field, is (Ruggiero et al. 2001)

$$W = \text{setup} + \text{runup} = CH_s, \tag{1}$$

where H_s is the offshore significant wave height and W is the sum of the magnitude of the wave setup (steady) and runup (unsteady), each of which has been suggested to depend on H_s. The cross-shore location of the W-defined, uprush waterline is X. The objective is to define C conservatively so that spurious water points are rejected, but not so conservatively that larger than necessary swaths of subaerial beach are rejected. To account for the variations between passes (e.g., Fig. 1c), W was estimated for each lidar pass.

To find the waterline, lidar elevations were estimated at 2-m cross-shore and alongshore intervals along east–west cross-shore transects, with smoothing over a 5-m radius to reduce noise. On each cross-shore transect and for each pass and value of C, the lidar waterline was defined as the most shoreward point with a vertical elevation less than or equal to W. All raw lidar data points shoreward of the waterline cross-shore location X were selected as subaerial, exposed beach data. The

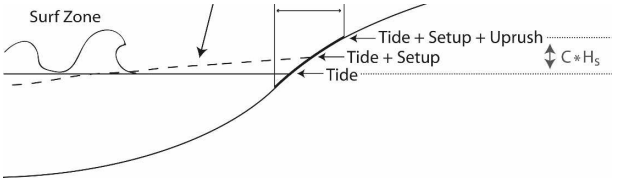

FIG. 2. Setup (dashed curve) elevates the mean water level above the local tide level (solid horizontal line). The swash excursion and vertical elevation reached by uprushes (CH_s above the tide level) and downrushes are also indicated.

passes were combined, yielding a set of beach face points and a set of ocean surface points. For the combined passes, the lidar shoreline was defined as the location of the most seaward beach data point (e.g., large green circle in Fig. 1d is for the optimal $C = 0.4$). Waterlines were found with C ranging from 0 to 0.6 in intervals of 0.1.

b. *Using in situ surveys*

Lidar and in situ vertical elevation data contained the mean (bias) and scatter errors inherent to GPS measurements. A net mean vertical offset was removed from the lidar data, where the offset was calculated as the mean elevation difference between lidar (all passes) and in situ (spanning a few days) data above the mean higher high water vertical datum, which was always well shoreward of the waterline. Offsets could have resulted from vertical GPS drift, or from changes in bathymetry during the completion time of the lidar and in situ surveys. The in situ data suggested that the bathymetry was not changing rapidly during the surveys. The largest offset was 15 cm, and in three of the five cases it was less than 4 cm (Table 1).

Based on repeat lidar and in situ surveys of piers, parking lots, U.S. Geological Survey (USGS) benchmarks, and other fixed targets, and using the same 1-m horizontal averaging cell size used here, expected RMS vertical differences between in situ and lidar surveys were about 21 cm. In situ and lidar surveys agree within the 21-cm error threshold on the subaerial beach and diverge seaward of the waterline, where the lidar survey does not measure the seafloor bathymetry (Figs. 1c,d, 3c, 4c, 6c). Using a smaller error threshold would include extraneous divergence points on the beach face instead of at the waterline, so this functional threshold was used.

The "true" waterline elevation W_{true} and cross-shore location X_{true} were defined for each pass as the elevation and cross-shore location where the in situ and lidar data diverge (black triangle in Figs. 3c, 4c, 6c). The divergence point was defined as the cross-shore location where the vertical difference between the two datasets was larger than the noise expected from sampling errors, rather than the actual wet–dry beach separation point. When the bathymetry is known, the divergence waterline locations, W_{true} and X_{true}, would be the lidar elevation and cross-shore location selected to identify subaerial beach data, whereas when the bathymetry is unknown, (1) is used to find W and X. Shoreward of X_{true}, even if the lidar is measuring the elevation of a thin tongue of water, the in situ and lidar elevation measurements are not distinguishable within the noise. The cross-shore location of the divergence waterline (X_{true}) is expected to vary alongshore, by about a swash excursion, as uprush and downrush are alternately sampled (Fig. 2).

4. Results

Two simple difference measures, horizontal and vertical, were used to select a single value of C that rejects lidar water returns from all passes, by comparing the divergence waterline (X_{true}, W_{true}) to the lidar waterlines (X, W for each value of C) for each pass.

The horizontal or cross-shore difference for each pass is $X_{\text{true}} - X$, the distance between the cross-shore location of the divergence waterline (X_{true}) and the most seaward point identified as the subaerial beach waterline (X) using tides and waves (1). Negative cross-shore differences are undesirable because they indicate that the lidar waterline is seaward of the divergence waterline, and water elevations are erroneously classified as subaerial beach (e.g., $C = 0$; magenta symbols in Figs. 4a, 6a). Large, positive cross-shore differences indicate that the lidar waterline is located far shoreward of the divergence waterline, and many subaerial beach elevations are eliminated because they are classified as water (e.g., $C = 0.6$; dark blue symbols; lidar waterlines are about 40 m shoreward of X_{true} in Figs. 3a, 4a, 6a). Alongshore variability of W_{true} and X_{true} within a pass is due to alongshore variation in the run-up phase (e.g., uprushes and downrushes), and possibly alongshore variation in the run-up amplitude. Beach slope and divergence waterline elevation (W_{true}) were not correlated (at the 5% significance level), suggesting that beach slope variations, which were small (0.01–0.04), did not significantly contribute to the alongshore variations in run-up amplitude. A single deep-water value of H_s was used to estimate W, and the alongshore variation of H_s was neglected.

The vertical or elevation difference for each pass is W minus the in situ elevation at the cross-shore location of the lidar waterline (X). When the lidar waterline (X) is erroneously located seaward of the divergence waterline (X_{true}), the elevation difference is positive and potentially large ($C = 0$; magenta symbols in Figs. 4b,c, 6b,c). When the lidar waterline is located at or shoreward of the divergence waterline, both in situ and lidar surveys are measuring sand level, or the lidar survey measures only a thin tongue of water, and their differences will be distributed around zero with scatter due to noise in both the lidar and in situ surveys, as seen for C values greater than zero in Fig. 3b.

Significant wave heights during lidar surveys ranged

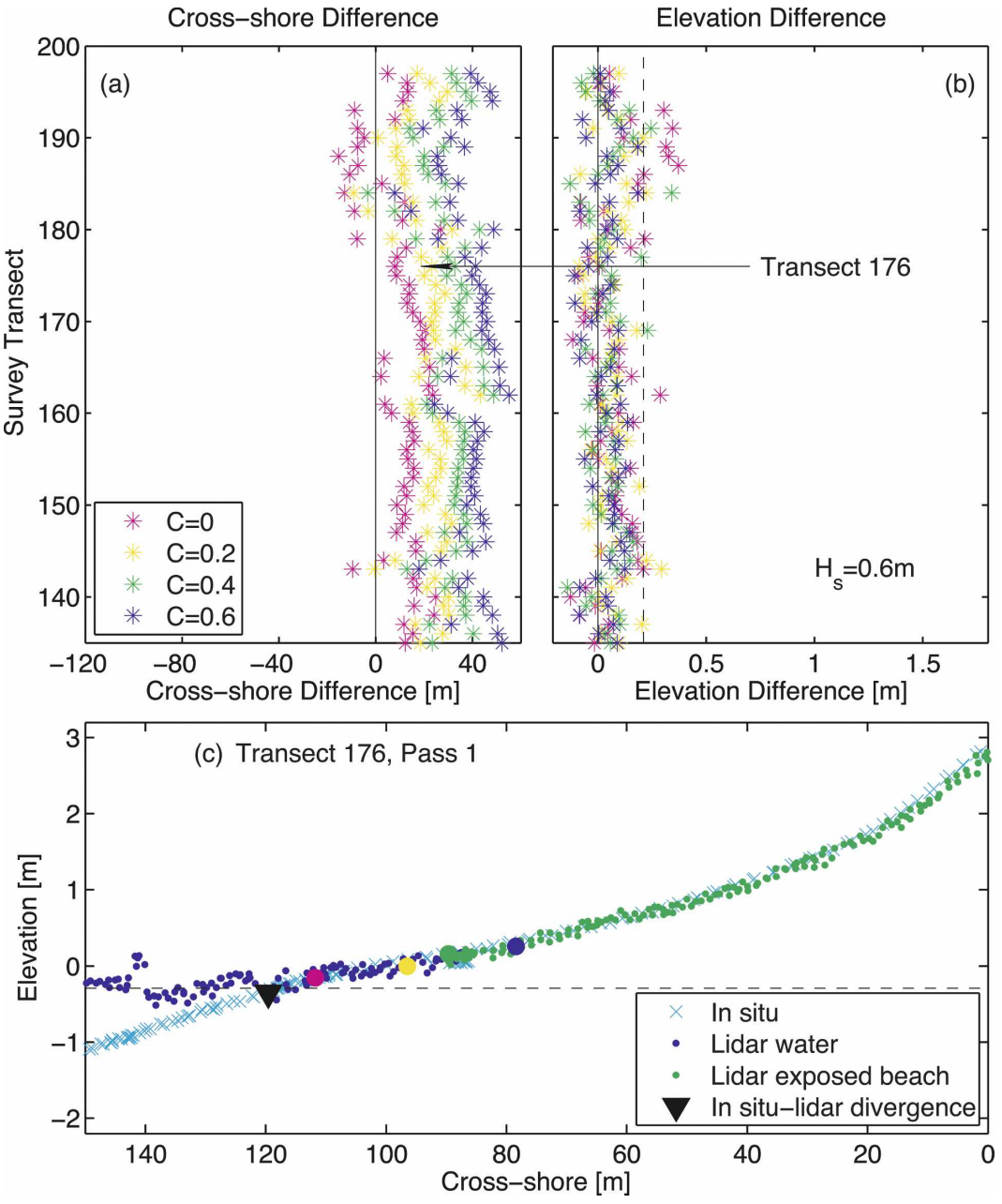

FIG. 3. Results for pass 1 in December 2002 along 65 in situ cross-shore survey transect lines. Wave heights were relatively low (H_s = 0.6 m). (a) Cross-shore (horizontal) difference ($X_{\text{true}} - X$) between the divergence waterline [X_{true}; black triangle in (c)] and the lidar waterline [X; large circles in (c)] estimated using tide and wave data (1). The colors correspond to C values ranging from 0 to 0.6 (for clarity, not all C are shown). (b) Elevation (vertical) difference between the lidar waterline (W) and in situ data at the cross-shore location (X) of the lidar waterline for different C. The vertical dashed line indicates the 21-cm elevation error threshold. (c) Elevation vs cross-shore location on transect line 176: in situ (blue x), lidar water (dark blue), and lidar subaerial beach (green), defined with C = 0.4 (1). For clarity, every other data point is shown. The dashed horizontal line is the tide level measured at the end of a nearby pier. Also shown are the divergence waterline (X_{true}; black triangle) and the lidar waterlines [X; large circles for different C values; same legend as in (a)].

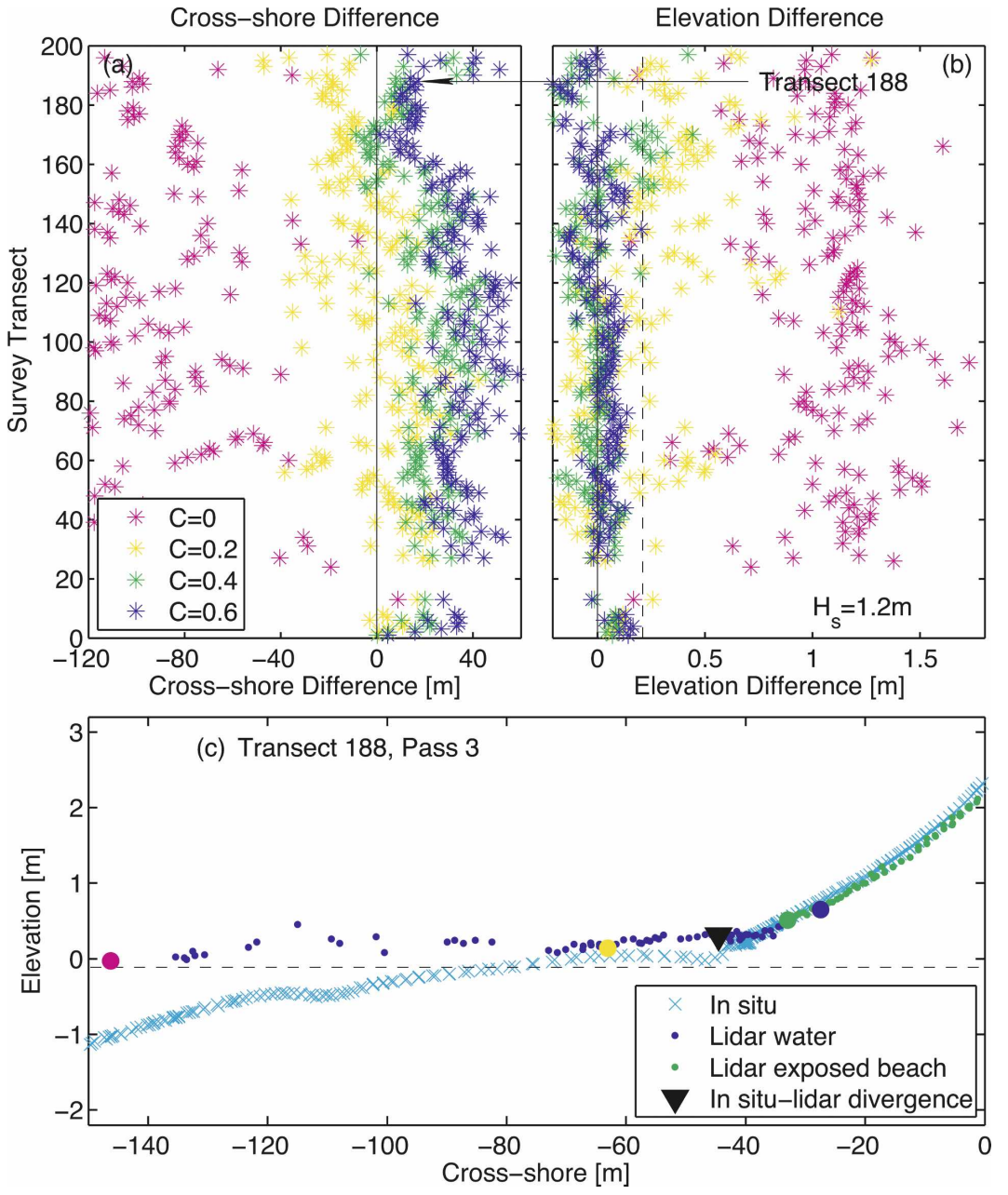

FIG. 4. Same format as in Fig. 3, but the results are for pass 3 in April 2004 on 199 cross-shore survey transect lines. Waves heights were relatively large (H_s = 1.2 m).

between 0.5 and 1.4 m. During the survey with the smallest wave height, wave setup and swash effects on the lidar waterline location were small (December 2002; H_s = 0.5–0.6 m; pass 1 shown in Fig. 3). Using C = 0 included only a few lidar water returns with negative values in Fig. 3a and elevation differences larger than 21 cm in Fig. 3b. For larger C, lidar waterline locations are shoreward of the divergence waterline (vertical solid line in Fig. 3a), and nearly all elevation differences are less than the 21-cm estimated noise threshold (vertical dashed line in Fig. 3b).

With large waves (April 2004; H_s = 1.2–1.3 m; Figs. 4, 6), wave setup and runup significantly affected the waterline location. With waves neglected (C = 0), points located more than 100 m seaward of the true waterline are misidentified as subaerial beach, and elevation errors are as large as 1.5 m (magenta symbols in Figs. 4a,b, respectively). Increasing C to 0.4 eliminates the

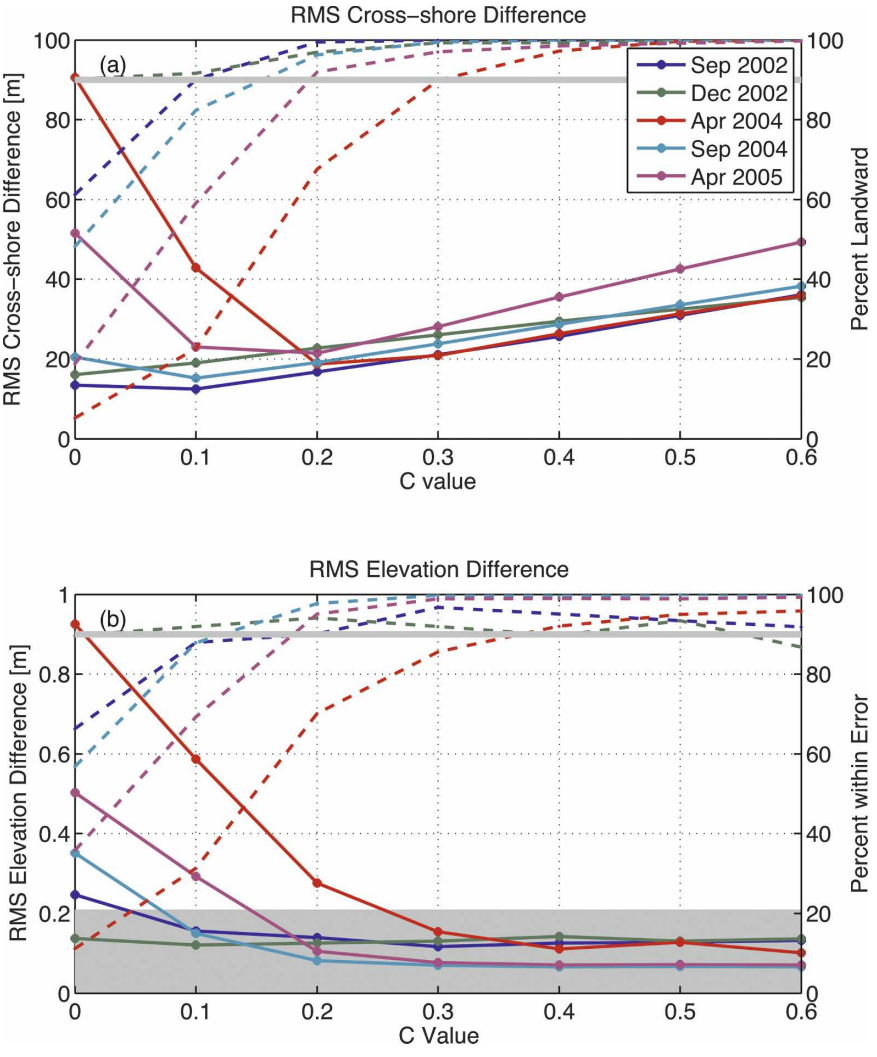

FIG. 5. Differences between in situ and lidar were used to select C. (a) RMS cross-shore differences between divergence (X_{true}) and lidar (X) waterline locations (solid lines, left axis), and percentage of lidar waterlines shoreward of the divergence waterline (dashed lines, right axis). (b) RMS elevation differences between the lidar waterline (W) and in situ data at the cross-shore location (X) of the lidar waterline (solid lines, left axis), and percentage of lidar waterlines within the 21-cm error threshold (dashed lines, right axis). The gray shaded area corresponds to elevation differences less than 21 cm. The gray horizontal lines in (a) and (b) indicate 90%.

lidar water returns, with vertical differences within the estimated noise threshold. Further increasing C excludes beach face data.

To select an overall C value, RMS cross-shore and elevation differences were calculated for each survey and C value (solid lines, Fig. 5). For small C and the largest wave heights (April 2004 and April 2005), the lidar waterline is seaward of the divergence waterline yielding large RMS cross-shore differences, and many water returns are erroneously classified as subaerial beach. For the largest C, the large RMS cross-shore differences indicate that the lidar waterline is located far landward of the divergence waterline, eliminating subaerial beach points. For intermediate C values, RMS cross-shore differences may be relatively small when the lidar waterline is slightly seaward or slightly shoreward of the divergence waterline. To distinguish between these two cases, the fraction of points shoreward of the divergence waterline was calculated for each survey and C value (dashed lines in Fig. 5a).

Elevation differences are large for small C when lidar water returns are included, and decrease with larger C to less than the 21-cm error threshold (within the shaded gray area in Fig. 5b). The percentage of lidar

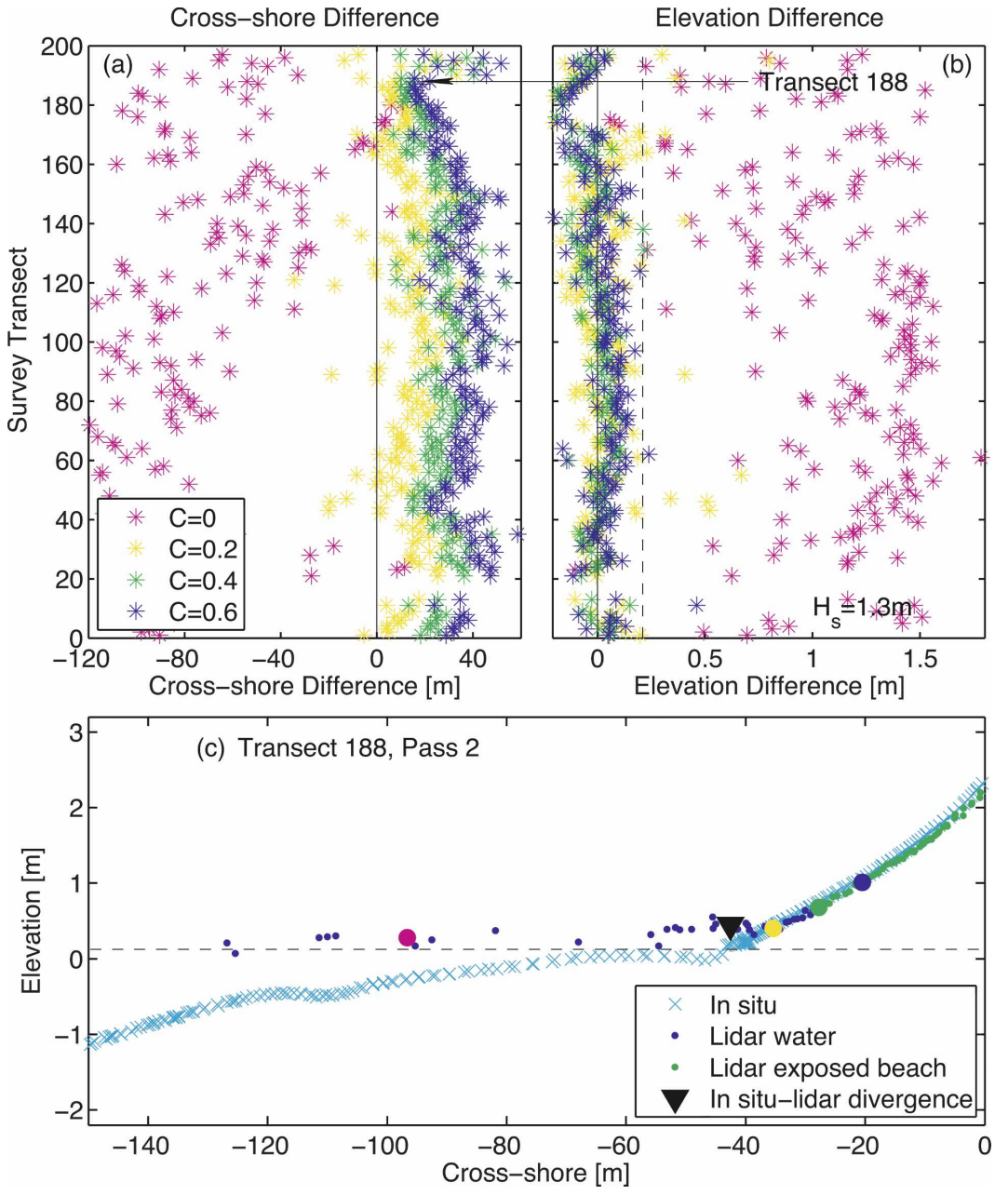

FIG. 6. Results for pass 2 in April 2004 on 199 cross-shore survey transect lines. Wave heights were relatively large (H_s = 1.3), but C = 0.2 is the optimal value, compared with C = 0.4 for pass 3 of the same survey (Fig. 4).

waterlines with elevation differences less than the error threshold also increases as C increases (dashed lines in Fig. 5b).

The optimal C value was selected for each survey as the smallest C with 90% of the retained lidar waterlines shoreward of the divergence waterline (X_{true}) and with 90% of the RMS elevation differences less than 21 cm. Optimal C ranged between 0 in December 2002, the day with the smallest waves, and 0.4 in April 2004, when waves were larger. The optimal C also varied within surveys. For example, in the April 2004 survey, the optimal value for pass 3 was C = 0.4 (Fig. 4), while for pass 2 it was C = 0.2 (Fig. 6).

A value of C = 0.4 removed water points from all surveys, while retaining most of the subaerial beach. With C = 0.4, the strip between X_{true} and X, rejected as water by the present algorithm, is between 26 and 36 m wide (Table 2). Reducing C would narrow this strip, but

TABLE 2. For each lidar survey (including between three and five passes), the range of elevation cutoffs (W), RMS horizontal difference between the cross-shore location of the $C = 0.4$ lidar waterline and the divergence waterline, and the RMS horizontal distance gained using the lidar waterline instead of the MHW contour are shown.

Survey	W range (m)	Cross-shore diff (m)	Distance MHW (m)
Sep 2002	0.60–0.66	26	47
Dec 2002	−0.13–0.63	29	68
Apr 2004	0.37–0.68	26	52
Sep 2004	0.49–1.05	29	57
Apr 2005	0.15–0.54	36	77

would increase the number of water data points that are included.

5. Discussion

a. Lidar return intensity and density

The intensity or strength of returns is increased by bubbles and foam (Mobley 1994), and individual breaking waves create bands of high intensity and high intensity gradients (not shown). However, the intensity also depends on scanning angle, decreasing with increasing angle (Mobley 1994). Simple methods based on intensity gradients approximately located the waterline along on some transects (not shown), but the results based on wave height and tide level (Table 2) were not improved by including intensity.

Similarly, on many cross-shore transects, the return density or points per square meter decreased seaward of the waterline (Fig. 6c). However, on some transects there was little or no decrease in point density near the waterline (Fig. 3c), and on other transects the variation in return density occurred farther offshore than the waterline (Fig. 4c), sometimes in the mid–surf zone (not shown). Previous studies suggest that the return density depends on the beam angle, as well as wind and wave conditions (Guenther et al. 2000; Krabill et al. 2000). The variation of return density across the surf zone and runup is not understood sufficiently to use for routine waterline identification.

b. Run-up and setup parameterizations

Equating W with $W_{2\%}$, the vertical level exceeded by 2% of wave runups, the corresponding $C_{2\%}$ is between roughly 0.4 and 0.5 (Ruggiero et al. 2001) on Oregon beaches with the Iribarren number (or surf similarity number) similar to Torrey Pines (between about 0.2 and 0.7). The Iribarren number, $\xi = \beta L_0^{1/2} H_0^{-1/2}$, where H_0 and L_0 are the deep-water wave height and wavelength and β is a representative beach slope (Battjes 1974), is widely used to characterize beaches. Small Iribarren numbers (less than about 1) denote dissipative beaches with spilling waves, and larger values correspond to reflective beaches with plunging or collapsing waves. Extensive field observations of the 2% exceedence runup suggest that $C_{2\%}$ depends on ξ (Holman 1986; Ruggiero et al. 2001; Stockdon et al. 2006), reaching values as high as three on steep beaches with low energy swell waves ($\xi \approx 3$). Alternative empirical formulations that relate $C_{2\%}$ to H_0/L_0 (without a β dependence) also suggest higher values of $C_{2\%}$ for a low energy swell (Ruggiero et al. 2001). In this study, with small ranges of wave height (0.5–1.4 m) and beach slope (0.01–0.04), the Iribarren number remained in the dissipative range, varying between 0.2 and 0.7. The Iribarren number or H_0/L_0, calculated for each pass, and the optimal C value were weakly correlated (squared coefficients of 0.4 and 0.3, respectively) at the 5% significance level. However, these correlations were determined with very few (19) data points with significant scatter, and would likely not be valid over a larger parameter range. To avoid retaining water points, increased values of C are recommended for the application of (1) to lidar obtained on beaches with significantly different waves and bathymetry than Torrey Pines. For example,

$$W_{2\%} = (0.83\xi + 0.2)H_s \tag{2}$$

(Holman 1986) overpredicts W at Torrey Pines, but is valid at large ξ.

Setup and runup depend on wave transformation across the surf zone. As the tide level changes and incident wave conditions remain relatively stable, the effective surf zone bathymetry and wave transformation change. For example, a sandbar that causes wave breaking at low tide can be too deep to induce breaking at high tide (Raubenheimer et al. 2001). Infragravity wave energy levels, which can dominate swash (runup) on dissipative beaches, also depend on the tide level and the associated variations in the effective surf zone bathymetry (Thomson et al. 2006). Simple parameterizations of setup and runup used to estimate $W_{2\%}$, for example (2), are therefore necessarily of limited accuracy. Nevertheless, empirical formulations for $W_{2\%}$ provide useful estimates of W for a wide range of beach and wave conditions.

6. Summary

Coastal lidar data include elevations of the exposed, subaerial beach and, seaward of the waterline, the ocean surface. Here, a simple method was developed to

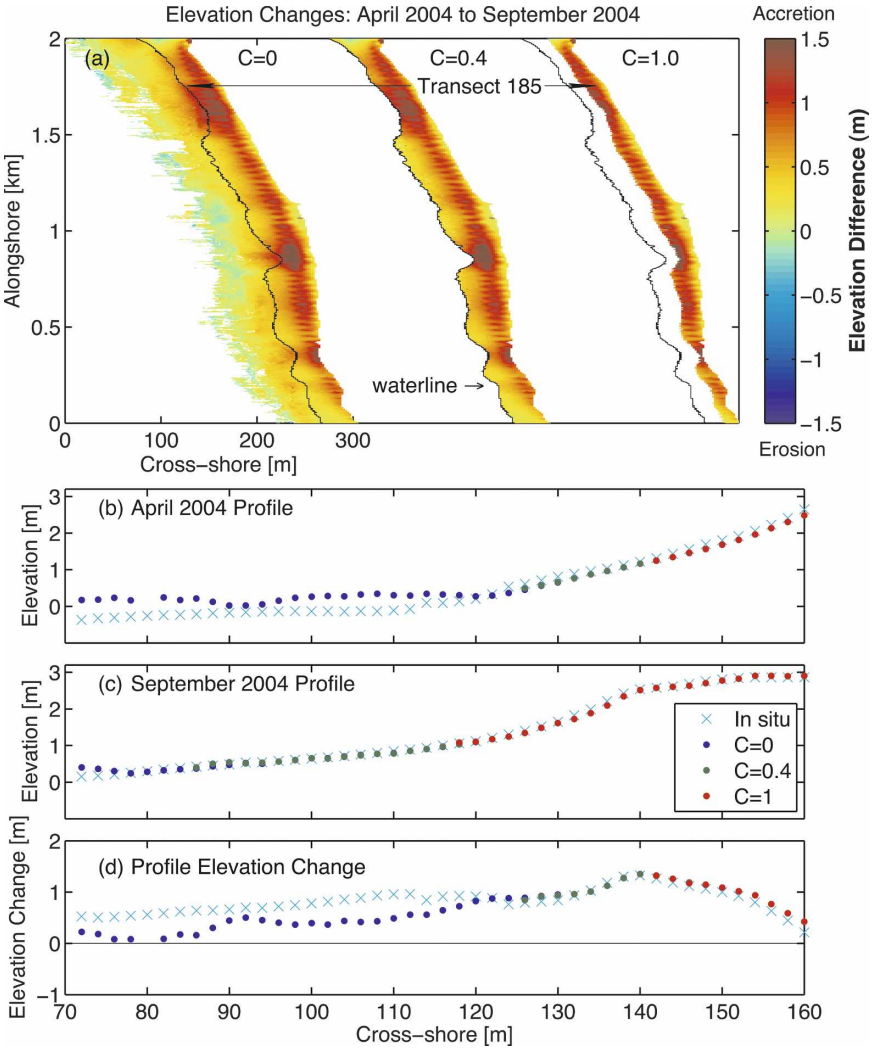

FIG. 7. (a) Plan view of beach sand level changes along 2 km of Torrey Pines State Beach from April 2004 to September 2004, estimated with lidar waterlines calculated using $C = 0, 0.4$, and 1.0 (left to right). Color scale is to the right. Each strip shows change between the cliffs bordering the backbeach (to the right) and the estimated waterline (to the left). The thin black curve superimposed on each change map corresponds to the lidar waterline with $C = 0.4$. Elevation vs cross-shore location for transect 185 [location indicated in (a)] for the (b) April 2004 and (c) September 2004 surveys. Elevations are binned every 2 m. (d) Elevation change between April and September 2004, with in situ data (blue x) and lidar data [color indicates the C values; legend in (c)].

remove water returns. A vertical elevation cutoff was used with the waterline elevation (W) above the known tide level during each lidar pass, due to the superelevation from wave setup and runup, assumed proportional to the offshore significant wave height H_s($W = CH_s$). Spatial change maps using $C = 0$, 0.4, and 1 to estimate the lidar waterline are shown in Fig. 7a. An overly conservative estimate of setup and runup at Torrey Pines ($C = 1$) excludes many subaerial beach points, while $C = 0$ includes many water points (Fig. 7b) and yields spurious beach changes (dark blue points in Fig. 7d). Using $C = 0.4$ shows the desired result of excluding water points while retaining most subaerial beach points (green points in Figs. 7b–d).

The pass-by-pass processing, with lidar waterlines estimated for each pass, effectively combines surveys acquired at different tide levels and wave conditions (Figs. 1c,d). Even though each survey spanned only 2 days and was centered around low tide, there was as much as a 0.7-m vertical difference in the lidar waterline elevation (W) and 34-m horizontal difference in the lidar waterline cross-shore location (X) between

passes (Table 2). Using $C = 0.4$ rather than MHW (sometimes used as a conservative default shoreline level, well above the waterline) added between (RMS) 47 and 77 m to the width of the subaerial beach (Table 2). The range of wave and beach conditions at Torrey Pines was limited. For application at beaches with waves or slopes very different than Torrey Pines, existing empirical formulas for C based on observations of setup and runup spanning a wide range of conditions [e.g., (2)] are recommended.

Acknowledgments. Lidar and in situ surveys were supported by the U.S. Army Corps of Engineers. Wave data collection was supported by the California Department of Boating and Waterways. Brian Woodward, Kent Smith, Dennis Darnell, and Bill Boyd collected the in situ bathymetry data. Marissa Yates was supported by a National Defense Science and Engineering Graduate Fellowship. A reviewer provided helpful suggestions.

REFERENCES

Battjes, J., 1974: Surf similarity. *Proc. 14th Conf. on Coastal Engineering,* Copenhagen, Denmark, American Society of Civil Engineers, 466–480.

Brock, J., C. Wright, A. Sallenger, W. Krabill, and R. Swift, 2002: Basis and methods of NASA Airborne Topographic Mapper lidar surveys for coastal studies. *J. Coastal Res.,* **18,** 1–13.

Gares, P., Y. Wang, and S. White, 2006: Using LIDAR to monitor a beach nourishment project at Wrightsville Beach, North Carolina, USA. *J. Coastal Res.,* **22,** 1206–1219.

Guenther, G., A. Cunningham, P. LaRocque, and D. Reid, 2000: Meeting the accuracy challenge in airborne lidar bathymetry. *Proc. 20th EARSeL Symp.: Workshop on Lidar Remote Sensing of Land and Sea,* Dresden, Germany, European Association of Remote Sensing Laboratories, 1.

Holman, R., 1986: Extreme value statistics for wave run-up on a natural beach. *Coastal Eng.,* **9,** 527–544.

Krabill, W., and Coauthors, 2000: Airborne laser mapping of Assateague National Seashore Beach. *Photogramm. Eng. Remote Sens.,* **66,** 65–71.

Mobley, C., 1994: *Light and Water: Radiative Transfer in Natural Waters.* Academic Press, 592 pp.

Morton, R., M. Leach, J. Paine, and M. Cardoza, 1993: Monitoring beach changes using GPS surveying techniques. *J. Coastal Res.,* **9,** 702–720.

Raubenheimer, B., R. Guza, and S. Elgar, 2001: Field observations of wave-driven setdown and setup. *J. Geophys. Res.,* **106,** 4629–4638.

Revell, D., P. Komar, and A. Sallenger, 2002: An application of LIDAR to analyses of El Niño erosion in the Netarts littoral cell, Oregon. *J. Coastal Res.,* **18,** 792–801.

Robertson, W., K. Zhang, and D. Whitman, 2007: Hurricane-induced beach change derived from airborne laser measurements near Panama City, Florida. *Mar. Geol.,* **237,** 191–205.

Ruggiero, P., P. Komar, W. McDougal, J. Marra, and R. Beach, 2001: Wave runup, extreme water levels and the erosion of properties backing beaches. *J. Coastal Res.,* **17,** 407–419.

Sallenger, A., W. Krabill, J. Brock, R. Swift, S. Manizade, and H. Stockdon, 2002: Sea-cliff erosion as a function of beach changes and extreme wave runup during the 1997–1998 El Niño. *Mar. Geol.,* **187,** 279–297.

——, and Coauthors, 2003: Evaluation of airborne topographic lidar for quantifying beach changes. *J. Coastal Res.,* **19,** 125–133.

Saye, S., D. van der Wal, K. Pye, and S. Blott, 2005: Beach-dune morphological relationships and erosion/accretion: An investigation at five sites in England and Wales using LIDAR data. *Geomorphology,* **72,** 128–155.

Seymour, R., R. Guza, W. O'Reilly, and S. Elgar, 2005: Rapid erosion of a small southern California beach fill. *Coastal Eng.,* **52,** 151–158.

Shrestha, R., W. Carter, M. Sartori, B. Luzum, and K. Slatton, 2005: Airborne laser swath mapping: Quantifying changes in sandy beaches over time scales of weeks to years. *Photogramm. Eng. Remote Sens.,* **59,** 222–232.

Stockdon, H., A. Sallenger, J. List, and R. Holman, 2002: Estimation of shoreline position and change using airborne topographic lidar data. *J. Coastal Res.,* **18,** 502–513.

——, R. Holman, P. Howd, and A. Sallenger, 2006: Empirical parameterization of setup, swash, and runup. *Coastal Eng.,* **53,** 573–588.

Thomson, J., S. Elgar, B. Raubenheimer, T. Herbers, and R. Guza, 2006: Tidal modulation of infragravity wave via nonlinear energy losses in the surfzone. *Geophys. Res. Lett.,* **33,** L05601, doi:10.1029/2005GL025514.

Wehr, A., and U. Lohr, 1999: Airborne laser scanning—an introduction and overview. *Photogramm. Eng. Remote Sens.,* **54,** 68–82.

Woolard, J., and J. Colby, 2002: Spatial characterization, resolution, and volumetric change of coastal dunes using airborne LIDAR: Cape Hatteras, North Carolina. *Geomorphology,* **48,** 269–287.

Young, A., and S. Ashford, 2006: Application of airborne LIDAR for seacliff volumetric change and beach-sediment budget contributions. *J. Coastal Res.,* **22,** 307–318.

Zhang, K., D. Whitman, S. Leatherman, and W. Robertson, 2005: Quantification of beach changes caused by Hurricane Floyd along Florida's Atlantic Coast using airborne laser surveys. *J. Coastal Res.,* **21,** 123–134.